

A Compact Dual-Band Rectenna Using Slot-Loaded Dual Band Folded Dipole Antenna

Kyriaki Niotaki, *Student Member, IEEE*, Sangkil Kim, *Student Member, IEEE*, Seongheon Jeong, *Member, IEEE*, Ana Collado, *Senior Member, IEEE*, Apostolos Georgiadis, *Senior Member, IEEE*, and Manos M. Tentzeris, *Fellow, IEEE*

Abstract—A compact dual-band rectenna operating at 915 MHz and 2.45 GHz is presented. The rectenna consists of a slot-loaded dual-band folded dipole antenna and a dual-band rectifier. The length of the proposed antenna is only 36.6% of the half-wavelength ($\lambda_0/2$) dipole antenna at 915 MHz while keeping dual-band property at 915 MHz and 2.45 GHz. The rectifier circuit is optimized for low input power densities using harmonic balance (HB) simulation. The efficiencies of the rectifier are evaluated with both single- and dual-frequency input signals. The measured results show an efficiency of 37% and 30% at 915 MHz and at 2.45 GHz when illuminated by a microwave signal of available power of -9 dBm for a load resistor of 2.2 k Ω .

Index Terms—Dipole antenna, dual-band rectenna, dual-band rectifier, energy harvesting, wireless power transmission.

I. INTRODUCTION

WIRELESS power transmission has received special attention recently for the implementation of low-cost and low-power battery-less operated sensors [1]. Since ambient energy is available in many frequency bands, RF energy harvesters capable of operating in multiple bands are of great importance. Nowadays, various approaches for designing rectennas have been considered in the literature including single-band operation [2], [3], broadband approaches [4], and multiband designs [5]–[7].

A compact wireless energy harvester (WEH) that is able to harvest power from a 915-MHz and a 2.45-GHz wireless source is presented in this letter. In a first step, the antenna and the rectifier are designed separately. Then, the rectenna element is optimized by jointly simulating the antenna and the rectifier using harmonic balance (HB) simulation.

Manuscript received August 23, 2013; revised October 31, 2013; accepted November 26, 2013. Date of publication December 05, 2013; date of current version January 07, 2014. This work was supported by the Spanish Ministry of Economy and Competitiveness and FEDER funds under Project TEC2012-39143 and the EU Marie Curie under Project FP7-PEOPLE-2009-IAPP 251557.

K. Niotaki, A. Collado, and A. Georgiadis are with the Department of Microwave Systems and Nanotechnology, Centre Tecnologic de Telecomunicacions de Catalunya (CTTC), 08860 Castelldefels, Spain (e-mail: nkiriaki@gmail.com; acollado@cttc.es; ageorgiadis@cttc.es).

S. Kim and M. M. Tentzeris are with the School of Electrical and Computer Engineering, Georgia Institute of Technology, Atlanta, GA 30332-250 USA (e-mail: ksangkil3@gatech.edu; etentze@ece.gatech.edu).

S. Jeong is with BlackBerry, Ltd., Irving, TX 75039 USA (e-mail: sjeong@ieee.org).

Color versions of one or more of the figures in this letter are available online at <http://ieeexplore.ieee.org>.

Digital Object Identifier 10.1109/LAWP.2013.2294200

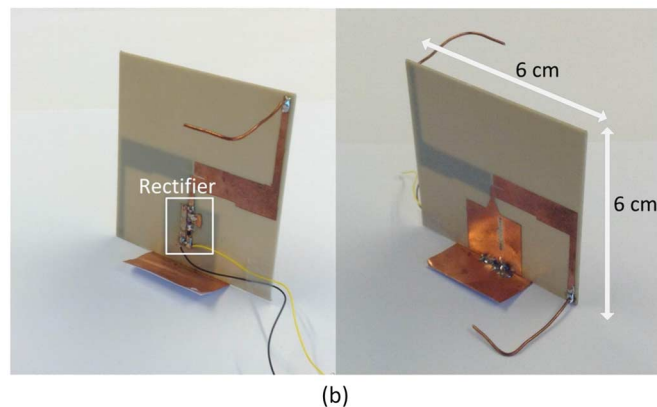
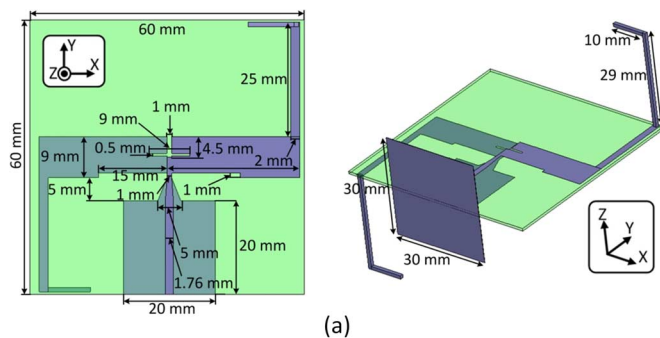


Fig. 1. Folded dipole antenna: (a) design of the top and side view and (b) fabricated rectenna.

The outline of this letter is as follows. In Section II, the dual-band folded dipole antenna design is presented. In Section III, HB simulation is used in a commercial simulator to optimize the rectifier efficiency at the frequency bands of interest. Measured results of the fabricated rectenna are presented, and a comparison to the state-of-the-art designs of multiband rectenna circuits is offered.

II. DUAL-BAND DIPOLE ANTENNA DESIGN

Initially, a dual-band antenna is designed using a full-wave finite element method (FEM) software tool (ANSYS HFSS) aside from a rectifier. The designed antenna topology is a slot-loaded dual-band folded dipole antenna fabricated on Arlon 25N substrate that has relative permittivity of 3.38 and loss tangent of $2.5 \cdot 10^{-3}$ utilizing a milling machine (LPKF ProtoMat E33, OR, USA [8]).

A simple half-wavelength ($\lambda_0/2$) dipole antenna at 915 MHz is folded to miniaturize the antenna, and a slot is loaded in

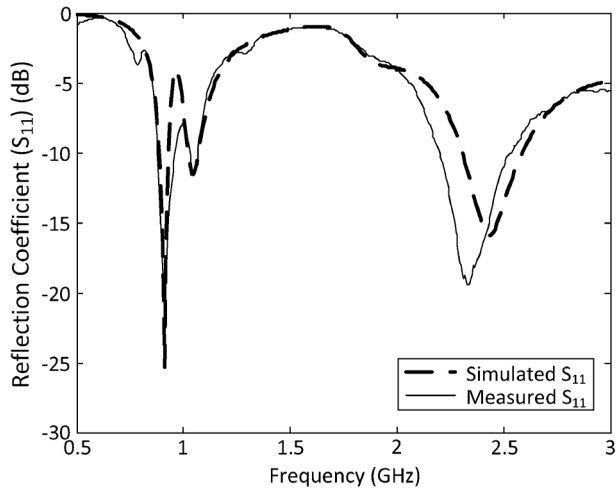


Fig. 2. Simulated and measured reflection coefficients (S_{11}) of the slot-loaded dual-band folded dipole antenna versus frequency.

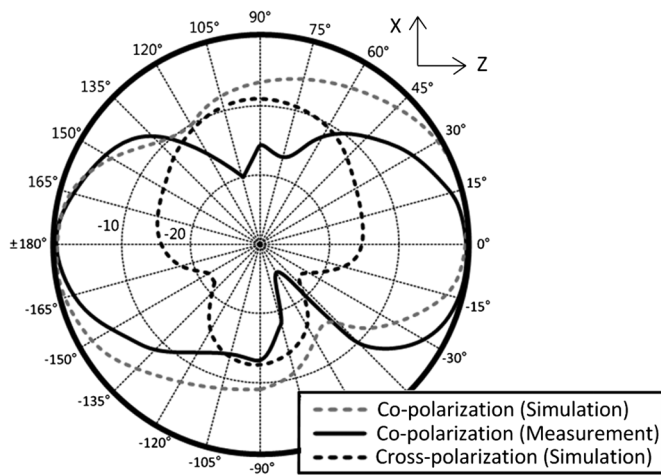


Fig. 3. Simulated and measured radiation pattern at 2.45 GHz (xz -plane).

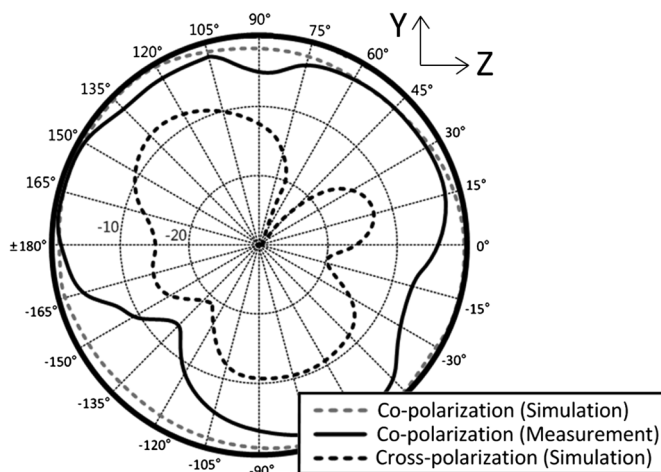


Fig. 4. Simulated and measured radiation pattern at 2.45 GHz (yz -plane).

the middle of the antenna to introduce the second resonant frequency at 2.45 GHz. The geometry of the designed antenna, as well as the fabricated prototype, is shown in Fig. 1.

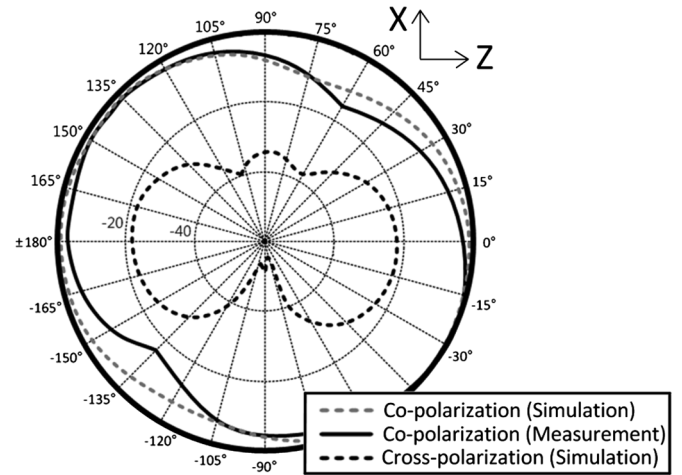


Fig. 5. Simulated and measured radiation pattern at 915 MHz (xz -plane).

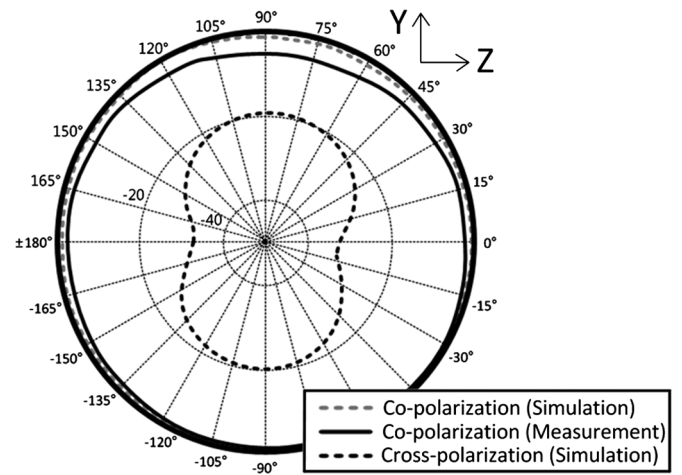


Fig. 6. Simulated and measured radiation pattern at 915 MHz (yz -plane).

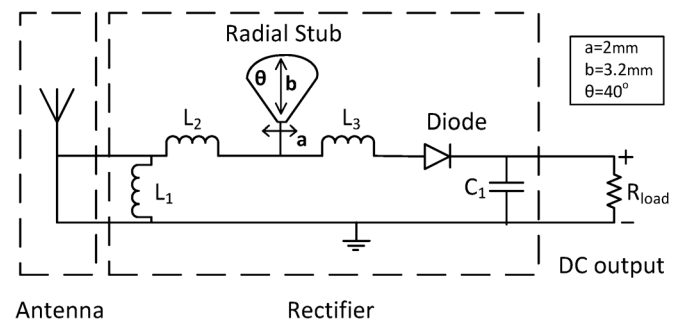


Fig. 7. Schematic of the proposed dual-band rectifier. Component values are $L_1 = 7.5$ nH, $L_2 = 10$ nH, $L_3 = 8.7$ nH, $C_1 = 100$ pF, and $R_{load} = 2.2$ k Ω .

The simulated and measured reflection coefficients (S_{11}) of the linearly polarized antenna are presented in Fig. 2, and the results demonstrate the 10-dB bandwidths cover the desired operation frequencies of 915 MHz and 2.45 GHz. The final size of the designed antenna is $6 \times 6 \times 6$ cm³ in a substrate thickness of 0.76 mm (30 mil). The measured antenna gains are 1.87 and 4.18 dBi at 915 MHz and 2.45 GHz, respectively. The measured and simulated radiation patterns for the xz - and yz -plane at 2.45 GHz and 915 MHz are shown in Figs. 3–6. Please note

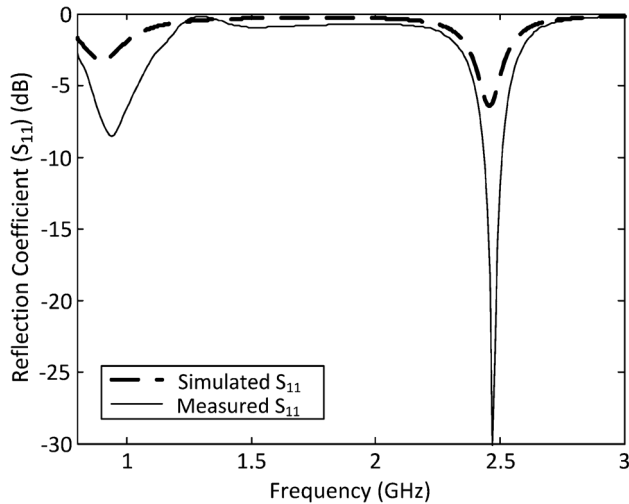


Fig. 8. Simulated and measured input reflection coefficient (S_{11}) of the dual-band rectifier versus frequency.

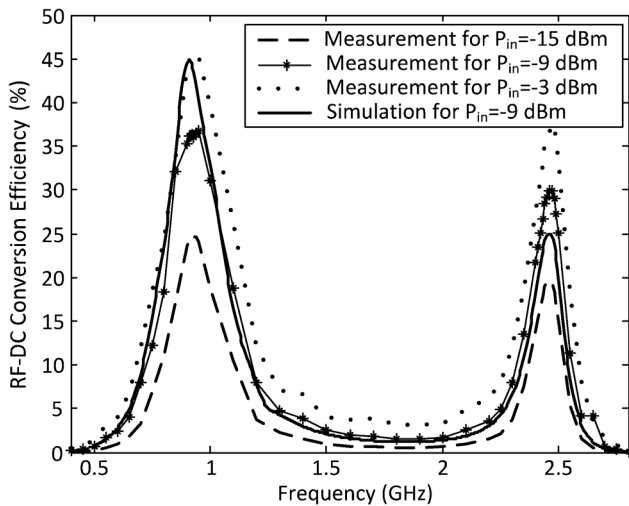


Fig. 9. Measured and simulated RF-DC conversion efficiency for various RF input power levels ($R_{load} = 2.2 \text{ k}\Omega$).

that copolarization corresponds to E_θ at xz -plane and E_φ at yz -plane.

III. DUAL-BAND RECTENNA DESIGN

As far as the targeted input power levels are low, a topology with only one rectifying device is selected as this has shown to lead to better RF-DC conversion efficiency [9] (Fig. 7). Agilent ADS HB simulation and optimization goals are used to maximize the RF-to-DC conversion efficiency at 915 MHz and 2.45 GHz. The goals are used to define the minimum RF-DC efficiency at 915 MHz and 2.45 GHz for a selected input power level and for an output load of 2.2 k Ω [9]. The optimum matching network consists of three inductances ($L_1 = 7.5 \text{ nH}$, $L_2 = 10 \text{ nH}$, and $L_3 = 8.7 \text{ nH}$) and a radial stub. The input impedance of the rectifier is matched to a 50- Ω representing the dipole antenna. The Skyworks SMS7630 Schottky diode is used for the design of the rectifier circuit. A prototype is built, and its performance is evaluated using single-tone as well as

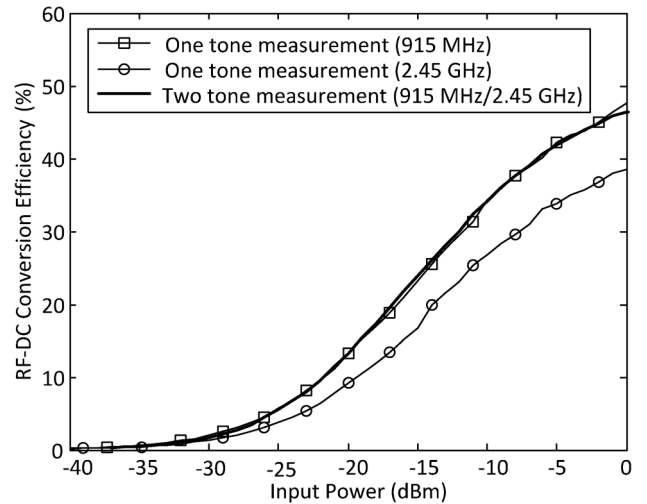


Fig. 10. Measured RF-DC conversion efficiency versus input power level for one-tone and dual-tone excitation ($R_{load} = 2.2 \text{ k}\Omega$).

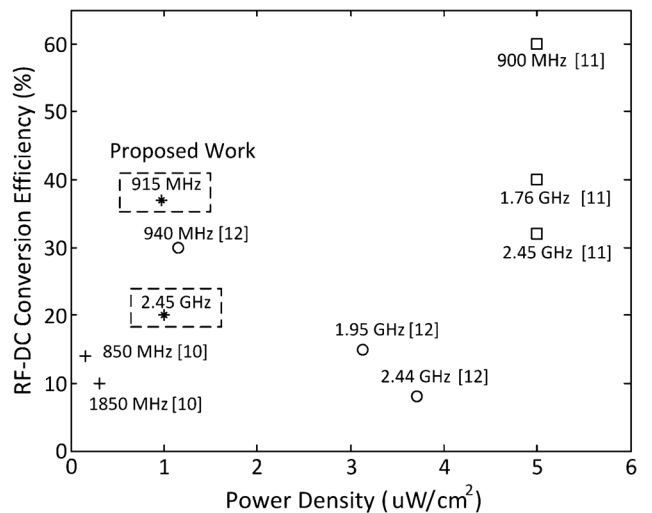


Fig. 11. Comparison of state-of-the-art designs of multiband rectenna circuits [10]–[12] to the proposed work.

dual-tone signal measurements. The total size of the rectifier is about $1.9 \times 2.1 \text{ cm}^2$. Simulated and measured reflection coefficient are shown in Fig. 8.

A comparison of the simulated and the measured values of the RF-DC conversion efficiency versus operating frequency for input power levels of -15 , -9 , and -3 dBm is shown in Fig. 9. Measurement results of the rectifier when harvesting simultaneously two equal-power tones from two RF sources at 915 MHz and 2.45 GHz are depicted in Fig. 10. The RF input signals are summed up by a power combiner at the input of the rectifier. The performance of the rectifier for one-tone and two-tone input signals at the frequencies of interest is compared for different input power levels in Fig. 10, showing an RF-DC conversion efficiency of 48% and 39% for an input power level of 0 dBm at 915 MHz and 2.45 GHz, respectively. Additionally, it can be seen that the rectifier RF-DC conversion efficiency is less than 1% for input power level lower than -33 dBm , as for this input power levels the Schottky diode is not operating in its optimum zone for maximum RF-DC conversion.

The rectenna is also evaluated for an incident power density of $1 \mu\text{W}/\text{cm}^2$. Considering the measured antenna gain at 915 MHz and 2.45 GHz, the antenna effective area is calculated as 132 and 31 cm^2 , respectively. For a power density of $1 \mu\text{W}/\text{cm}^2$, the input power is -9 and -15 dBm at 915 MHz and at 2.45 GHz, resulting in an RF–DC conversion efficiency of 37% and 20%, respectively. Fig. 11 depicts a comparison of the proposed work to a selection of state-of-the-art multiband rectenna designs showing improved performance for low power density levels.

REFERENCES

- [1] R. Vyas, V. Lakafosis, A. Rida, N. Chaisilwattana, S. Travis, J. Pan, and M. M. Tentzeris, "Paper-based RFID-enabled wireless platforms for sensing applications," *IEEE Trans. Microw. Theory Tech.*, vol. 57, no. 5, pp. 1370–1382, May 2009.
- [2] A. Costanzo, M. Fabiani, A. Romani, D. Masotti, and V. Rizzoli, "Co-design of ultra-low power RF/microwave receivers and converters for RFID and energy harvesting applications," in *Proc. IEEE MTT-S Int. Microw. Symp.*, Anaheim, CA, USA, May 23–28, 2010, pp. 856–859.
- [3] Y.-J. Ren and K. Chang, "5.8-GHz circularly polarized dual-diode rectenna and rectenna array for microwave power transmission," *IEEE Trans. Microw. Theory Tech.*, vol. 54, no. 4, pp. 1495–1502, Jun. 2006.
- [4] J. A. Hagerty, F. B. Helmbrecht, W. H. McCalpin, R. Zane, and Z. B. Popovic, "Recycling ambient microwave energy with broad-band rectenna arrays," *IEEE Trans. Microw. Theory Tech.*, vol. 52, no. 3, pp. 1014–1024, Mar. 2004.
- [5] H.-K. Chiou and I.-S. Chen, "High-efficiency dual-band on-chip rectenna for 35- and 94-GHz wireless power transmission in 0.13- μm CMOS technology," *IEEE Trans. Microw. Theory Tech.*, vol. 58, no. 12, pp. 3598–3606, Dec. 2010.
- [6] Y.-H. Suh and K. Chang, "A high-efficiency dual-frequency rectenna for 2.45- and 5.8-GHz wireless power transmission," *IEEE Trans. Microw. Theory Tech.*, vol. 50, no. 7, pp. 1784–1789, Jul. 2002.
- [7] G. De Vita and G. Iannaccone, "Design criteria for the RF section of UHF and microwave passive RFID transponders," *IEEE Trans. Microw. Theory Tech.*, vol. 53, no. 9, pp. 2978–2990, Sep. 2005.
- [8] LPKF, Garbsen, Gemany, "LPKF ProtoMat E33," [Online]. Available: <http://www.lpkfusa.com/protomat/e33.htm>
- [9] A. Boaventura, A. Collado, N. B. Carvalho, and A. Georgiadis, "Optimum behavior: Wireless power transmission system design through behavioral models and efficient synthesis techniques," *IEEE Microw. Mag.*, vol. 14, no. 2, pp. 26–35, Mar.–Apr. 2013.
- [10] A. Collado and A. Georgiadis, "Conformal hybrid solar and Electromagnetic (EM) energy harvesting rectenna," *IEEE Trans. Circuits Syst. I, Reg. Papers*, vol. 60, no. 8, pp. 2225, 2234, Aug. 2013.
- [11] V. Rizzoli, G. Bichicchi, A. Costanzo, F. Donzelli, and D. Masotti, "CAD of multi-resonator rectenna for micro-power generation," in *Proc. EuMIC*, Sep. 28–29, 2009, pp. 331–334.
- [12] B. L. Pham and A.-V. Pham, "Triple bands antenna and high efficiency rectifier design for RF energy harvesting at 900, 1900 and 2400 MHz," in *Proc. IEEE MTT-S Int. Microw. Symp.*, Seattle, WA, USA, Jun. 2–7, 2013.